Short Article

Developmental Cell

A bipartite element with allele-specific functions safeguards DNA methylation imprints at the *Dlk1-Dio3* locus

Graphical abstract

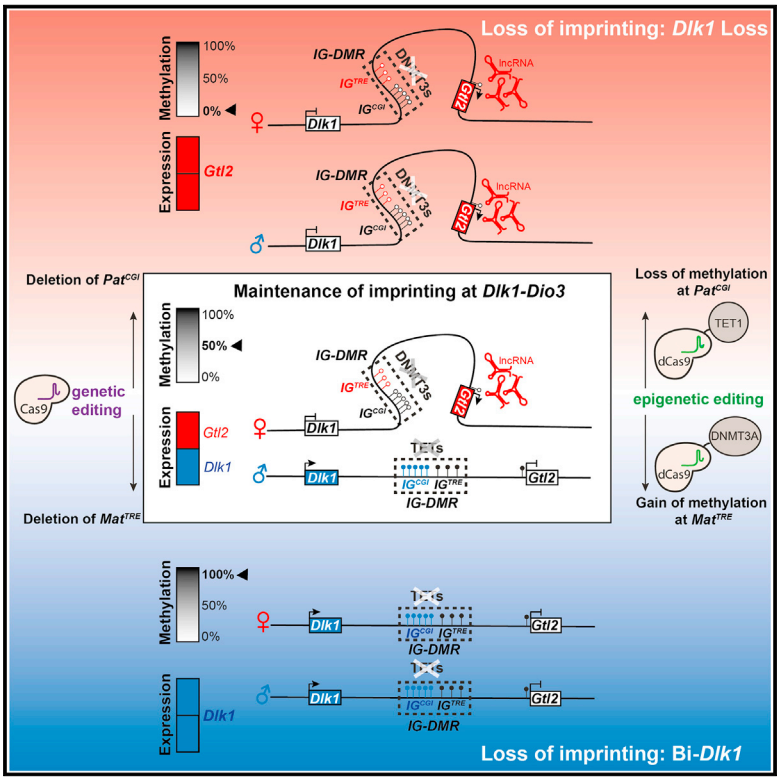

Highlights

- The IG-DMR is a bipartite element with distinct allele-specific functions
- A non-canonical enhancer within the IG-DMR prevents DNA methyltransferase activity
- Targeted epigenome editing allows induction of specific imprinting phenotypes
- CRISPRi reveals a functional hierarchy between DMRs that dictates imprint stability

Authors

Boaz E. Aronson, Laurianne Scourzic, Veevek Shah, ..., Meelad M. Dawlaty, Matthias Stadtfeld, Effie Apostolou

Correspondence

mas4011@med.cornell.edu (M.S.), efa2001@med.cornell.edu (E.A.)

In brief

Aronson et al. identify gene regulatory elements that ensure epigenetic stability at the major imprinted locus, Dlk1-Dio3, encoding essential developmental regulators. They show that these elements operate by counteracting *de novo* DNA methylation or demethylation in an allele-specific manner, providing a framework for epigenetic gene expression control.

Aronson et al., 2021, Developmental Cell *56*, 1–14
November 22, 2021
https://doi.org/10.1016/j.devcel.2021.10.004

CellPress

Please cite this article in press as: Aronson et al., A bipartite element with allele-specific functions safeguards DNA methylation imprints at the *Dlk1-Dio3* locus, Developmental Cell (2021), https://doi.org/10.1016/j.devcel.2021.10.004

Developmental Cell

CellPress

Short Article

A bipartite element with allele-specific functions safeguards DNA methylation imprints at the *Dlk1-Dio3* locus

Boaz E. Aronson,[1,15] Laurianne Scourzic,[1,15] Veevek Shah,[1] Emily Swanzey,[2,14] Andreas Kloetgen,[3,4] Alexander Polyzos,[1] Abhishek Sinha,[5] Annabel Azziz,[6] Inbal Caspi,[7] Jiexi Li,[1] Bobbie Pelham-Webb,[8] Rachel A. Glenn,[6,7,9] Thomas Vierbuchen,[7,9] Hynek Wichterle,[5,10] Aristotelis Tsirigos,[3,11] Meelad M. Dawlaty,[12,13] Matthias Stadtfeld,[2,*] and Effie Apostolou[1,16,*]

[1]Sanford I Weill Department of Medicine, Division of Hematology/Oncology, Sandra and Edward Meyer Cancer Center, New York, NY 10021, USA
[2]Sanford I Weill Department of Medicine, Division of Regenerative Medicine, Weill Cornell Medicine, New York, NY 10021, USA
[3]Department of Pathology, New York University School of Medicine, New York, NY 10016, USA
[4]Department of Computational Biology of Infection Research, Helmholtz Centre for Infection Research, 38124 Braunschweig, Germany
[5]Department of Pathology and Cell Biology, Columbia University Irving Medical Center, New York, NY 10032, USA
[6]Weill Cornell Graduate School of Medical Sciences, Weill Cornell Medicine, New York, NY 10065, USA
[7]Developmental Biology Program, Memorial Sloan Kettering Cancer Center, New York, NY 10065, USA
[8]Weill Cornell/Rockefeller/Sloan Kettering Tri-Institutional MD-PhD program, New York, NY, USA
[9]Center for Stem Cell Biology and Center for Epigenetics Research, Memorial Sloan Kettering Cancer Center, New York, NY 10065, USA
[10]Department of Neurology, Neuroscience and Rehabilitation and Regenerative Medicine, Columbia University Irving Medical Center, Center for Motor Neuron Biology and Disease and Columbia Stem Cell Initiative, Columbia University Irving Medical Center, New York, NY 10032, USA
[11]Institute for Computational Medicine and Applied Bioinformatics Laboratories, New York University School of Medicine, New York, NY 10016, USA
[12]Ruth L and David S. Gottesman Institute for Stem Cell and Regenerative Medicine Research, Bronx, NY 10461, USA
[13]Department of Genetics, Department of Developmental & Molecular Biology, Albert Einstein College of Medicine, Bronx, NY 10461, USA
[14]The Jackson Laboratory, Bar Harbor, ME, USA
[15]These authors contributed equally
[16]Lead contact
*Correspondence: mas4011@med.cornell.edu (M.S.), efa2001@med.cornell.edu (E.A.)
https://doi.org/10.1016/j.devcel.2021.10.004

SUMMARY

Loss of imprinting (LOI) results in severe developmental defects, but the mechanisms preventing LOI remain incompletely understood. Here, we dissect the functional components of the imprinting control region of the essential *Dlk1-Dio3* locus (called IG-DMR) in pluripotent stem cells. We demonstrate that the IG-DMR consists of two antagonistic elements: a paternally methylated CpG island that prevents recruitment of TET dioxygenases and a maternally unmethylated non-canonical enhancer that ensures expression of the *Gtl2* lncRNA by counteracting *de novo* DNA methyltransferases. Genetic or epigenetic editing of these elements leads to distinct LOI phenotypes with characteristic alternations of allele-specific gene expression, DNA methylation, and 3D chromatin topology. Although repression of the *Gtl2* promoter results in dysregulated imprinting, the stability of LOI phenotypes depends on the IG-DMR, suggesting a functional hierarchy. These findings establish the IG-DMR as a bipartite control element that maintains imprinting by allele-specific restriction of the DNA (de)methylation machinery.

INTRODUCTION

More than 100 mammalian genes, most of them found within coregulated clusters, are expressed in a mono-allelic, parent-of-origin-specific manner (Tucci et al., 2019). This phenomenon, referred to as genomic imprinting, is essential for mammalian development. Most imprinted expression is controlled by DNA methylation marks that are established in germ cells in a sex-specific manner at *cis*-regulatory differentially methylated regions (DMRs) called imprinting control regions (ICRs). DMRs within imprinted gene loci are subsequently acted upon by specific transcription factors (TFs) and chromatin modifiers to ultimately establish patterns of mono-allelic gene expression (Ferguson-Smith and Bourc'his, 2018). These epigenetic patterns are generally preserved in somatic cells throughout development and in adult tissues, and their dysregulation by loss of imprinting (LOI) can lead to fetal death or developmental abnormalities, as well as other disorders, such as cancer (Kalish et al., 2014). The mechanisms by which ICRs ensure retention of parent-of-origin DNA methylation,

Please cite this article in press as: Aronson et al., A bipartite element with allele-specific functions safeguards DNA methylation imprints at the *Dlk1-Dio3* locus, Developmental Cell (2021), https://doi.org/10.1016/j.devcel.2021.10.004

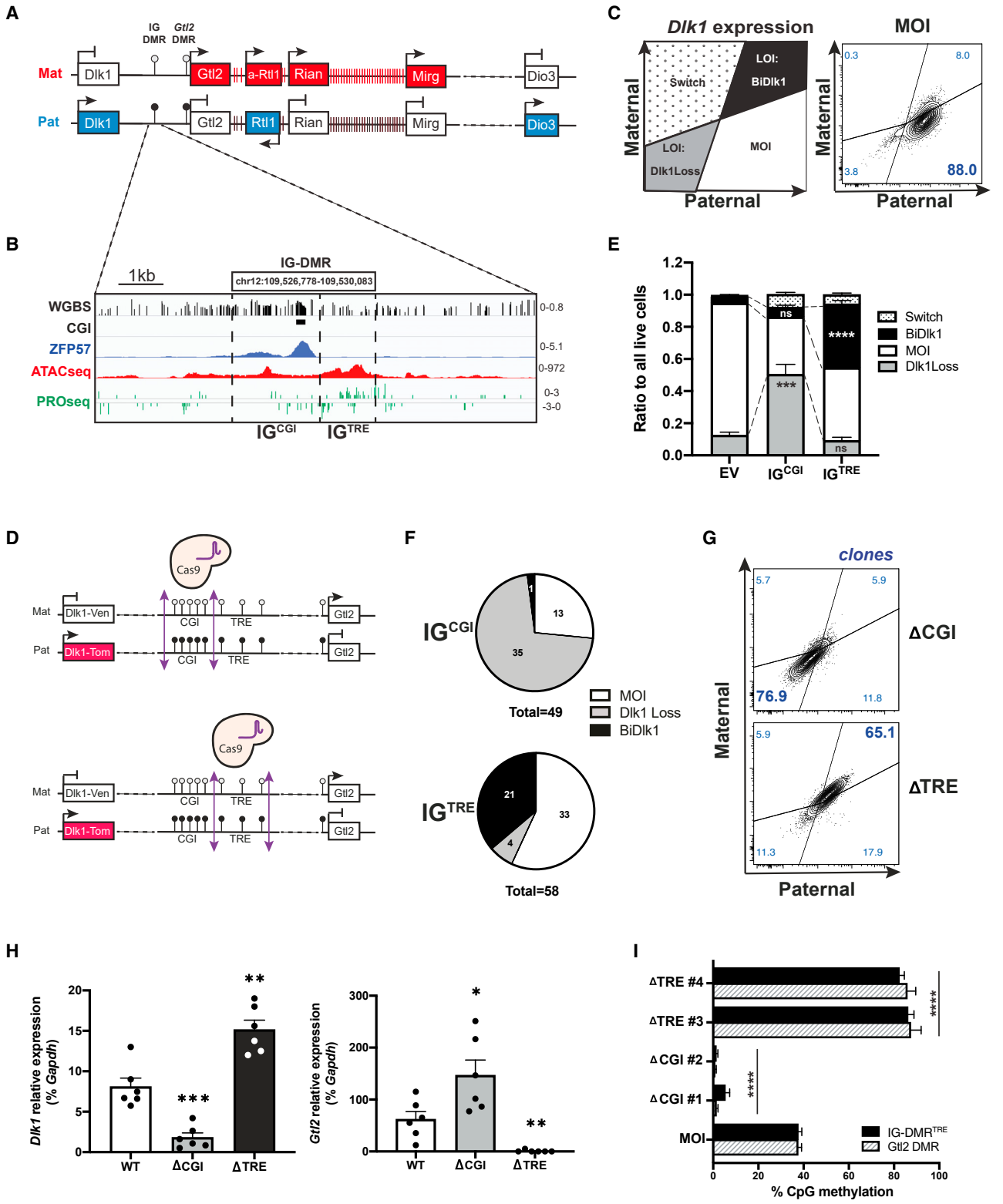

Figure 1. A bipartite IG-DMR element regulates genomic imprinting at *Dlk1-Dio3*

(A) Schematic representation of the murine *Dlk1-Dio3* locus highlighting maternally (red) and paternally (blue) expressed genes (not to scale). DMR, differentially methylated region; IG, intergenic; mat, maternal; pat, paternal. Lollipops represent DNA methylation state: dark, methylated; white, unmethylated.

(B) Distinct chromatin features of IG^{CGI} and IG^{TRE} (see also Figure S1A). IG-DMR coordinates (mm10) are boxed.

(legend continued on next page)

Please cite this article in press as: Aronson et al., A bipartite element with allele-specific functions safeguards DNA methylation imprints at the *Dlk1-Dio3* locus, Developmental Cell (2021), https://doi.org/10.1016/j.devcel.2021.10.004

known as maintenance of imprinting (MOI), remain incompletely understood.

The *Dlk1-Dio3* locus is a paradigmatic imprinted gene cluster that encodes multiple non-coding and coding transcripts within a region that spans almost one megabase of mouse chromosome 12 (da Rocha et al., 2008). LOI at *Dlk1-Dio3* is associated with severe developmental defects and aggressive malignancies (da Rocha et al., 2008; Jelinic and Shaw, 2007; Khoury et al., 2010; Manodoro et al., 2014) and can also occur during derivation and culture of induced pluripotent stem cells (iPSCs) (Carey et al., 2011; Liu et al., 2010; Stadtfeld et al., 2012; Mo et al., 2015) and embryonic stem cells (ESCs) (Stelzer et al., 2016; Swanzey et al., 2020), impairing their developmental potential. An intergenic DMR (IG-DMR), which resides between the maternally expressed *Gtl2* long non-coding RNA (lncRNA) and the paternally expressed *Dlk1* protein coding gene, has been shown to function as the ICR of *Dlk1-Dio3* locus (Lin et al., 2003). Similar to the *H19-Igf2* and *Rasgrf1* ICRs (Kobayashi et al., 2006; Yoon et al., 2005), the IG-DMR is methylated on the paternal allele and has been suggested to control methylation of the *Gtl2* promoter, a secondary DMR ("Gtl2 DMR") that exhibits paternal-specific methylation in post-implantation embryos and in cultured pluripotent cells (Sato et al., 2011; Stadtfeld et al., 2010) (Figure 1A).

Gtl2 has been shown to repress the maternal *Dlk1* gene in *cis* through recruitment of the polycomb repressive complex II (PRC2) (Zhao et al., 2010; Das et al., 2015; Kaneko et al., 2014; Sanli et al., 2018). This suggests that the control of *Gtl2* expression by the IG-DMR (Lin et al., 2003; Kota et al., 2014; Luo et al., 2016; Das et al., 2015) is essential for MOI at *Dlk1-Dio3*. However, it remains elusive as to how the IG-DMR achieves this regulation in an allele-specific manner. Targeted knockout of the IG-DMR (~4-kb region) in mice has shown that the transmission of maternal deletion results in LOI and specifically in paternalization of the maternal allele, including silencing of *Gtl2* and bi-allelic expression of *Dlk1* (Lin et al., 2003). However, transmission of the paternal deletion results in no phenotype (Lin et al., 2003; Das et al., 2015), which is surprising, given that the paternal IG-DMR becomes "imprinted" by DNA methylation in the male germline between embryonic days E15.5 to E16.5 (Sato et al., 2011; Nowak et al., 2011; SanMiguel and Bartolomei, 2018). Different phenotypes were recently reported upon deletion of a 216-bp tandem repeat CpG island (CGI) within the IG-DMR, where the repressive zinc-finger protein ZFP57 binds. Paternally transmitted deletion of this element resulted in maternalization of the paternal allele, whereas maternal transmission of the CGI deletion had no phenotype (Saito et al., 2018; Hara et al., 2019).

These apparently contradictory findings suggest that the IG-DMR might be a complex genomic element with multiple *cis*-regulatory regions that coordinate allele-specific gene expression. Therefore, we decided to dissect the molecular regulatory logic of imprint maintenance at *Dlk1-Dio3* in pluripotent stem cells (PSCs), a cell type that represents a tractable model system to investigate epigenetic mechanisms, including imprinting (Swanzey et al., 2020). Our results show that the IG-DMR is a bipartite element that maintains imprinting by stabilizing the germ-line-specific DNA methylation state at *Dlk1-Dio3*. This is achieved by the allele-specific function of two antagonistic *cis*-regulatory regions within the IG-DMR, which we propose to restrict the activity of DNA methyltransferases and dioxygenases and thereby operate as activator or repressor of the Gtl2 DMR, respectively. Allele-specific modulations of these elements were sufficient to induce specific and opposing expression phenotypes and epigenotypes, both indicative of LOI. Intriguingly, we observed that epigenetic repression of the *Gtl2* promoter caused bi-allelic *Dlk1* expression without affecting methylation at the IG-DMR. However, this LOI phenotype was unstable and reverted to MOI over time. Therefore, in addition to resolving the complex composition of the IG-DMR, our findings reveal previously unappreciated regulatory principles of the functional hierarchy between genomic elements operational in a gene cluster essential for mammalian development.

RESULTS

The IG-DMR is a bipartite element with two distinct functions

To gain insights into the regulatory mechanisms underlying the maintenance of *Dlk1-Dio3* imprinting (Figure 1A), we first assembled in-house (Di Giammartino et al., 2019; Liu et al., 2017; Pelham-Webb et al., 2021) and published datasets (Williams et al., 2011; Shi et al., 2019), including datasets from the CODEX database (Sánchez-Castillo et al., 2015) on DNA methylation, chromatin accessibility, nascent transcription, histone modifications, and TF-binding profiles at the IG-DMR in mouse ESCs (Takada et al., 2002; Kobayashi et al., 2006; Hiura et al., 2007). This revealed a pronounced dichotomy with respect to the position and nature of epigenomic features within the IG-DMR (chr12: 109,526,778–109,530,083 mm10) (Figures 1A, 1B, and S1A). The 2-kb region closer to the *Dlk1* gene exhibits high CpG density, including a CGI with conserved tandem repeats between human, mouse, and sheep (Paulsen et al., 2001), binding of the repressive KRAB domain containing zinc-finger protein ZFP57

(C) Schematic representation of distinct phenotypic populations detected by flow cytometry using the *Dlk1* reporter system shows an example of normal imprinted (MOI) cells (right).
(D) Schematic representation of IG^{CGI} and IG^{TRE} deletions.
(E) Relative ratios of specific *Dlk1* phenotypes in bulk populations after targeting either IG^{CGI} or IG^{TRE}. n = 8 for empty vector control (EV), n = 8 for IG^{CGI}, and n = 6 for IG^{TRE}. Significance relative to EV (dashed lines) was calculated using a two-tailed unpaired Student's t test.
(F) Frequency of indicated phenotypes in clonal cell lines after targeting either IG^{CGI} or IG^{TRE}.
(G) FACS plots of clonal lines with LOI-Dlk1Loss and LOI-BiDlk1 phenotypes and confirmed deletion of IG^{CGI} (ΔCGI) and IG^{TRE} (ΔTRE), respectively.
(H) qRT-PCR analysis of *Dlk1* and *Gtl2* expression relative to *Gapdh* in retinoic acid (RA)-differentiated clones (n = 6) with indicated genotypes. Statistical significance relative to WT was calculated using a two-tailed unpaired Student's t test.
(I) Percent DNA methylation at individual CpG resolution in iPSCs at the IG-DMR and the Gtl2 DMR as assessed by pyrosequencing; "region 2" ($IG\text{-}DMR^{TRE}$) and "region 3" (Gtl2 DMR) (see STAR Methods for coordinates). Note that region 2 is ~300 bp outside of the region deleted by Cas9. n = 2 clones per genotype are represented. Two-tailed paired Student's t test was used to calculate significance relative to MOI levels. For all panels: asterisks indicate significance: *$p \leq 0.05$, **$p \leq 0.01$, ***$p \leq 0.001$, ****$p \leq 0.0001$. n.s, not significant. Error bars represent ± SEM. See statistics summarized in Table S4.

Please cite this article in press as: Aronson et al., A bipartite element with allele-specific functions safeguards DNA methylation imprints at the *Dlk1-Dio3* locus, Developmental Cell (2021), https://doi.org/10.1016/j.devcel.2021.10.004

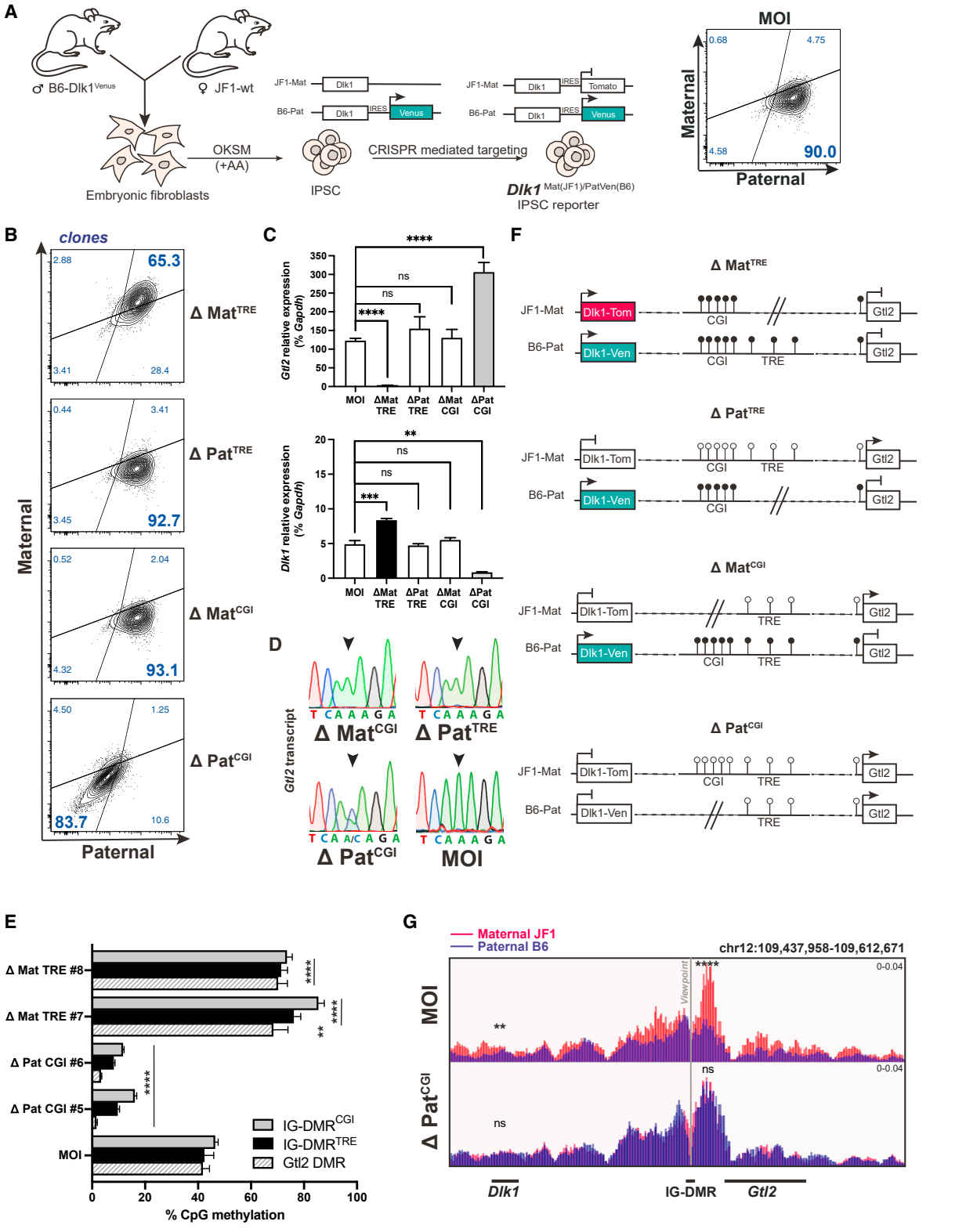

Figure 2. Dual role of IG-DMR in allele-specific regulation of *Dlk1-Dio3* locus

(A) Schematic of insertion of an IRES-tdTomato cassette into the maternal *Dlk1* allele and validation of MOI in resultant B6xJF1 hybrid reporter iPSCs. OKSM, OCT4, KLF4, SOX2, and MYC; AA, ascorbic acid.

(B) Representative FACS plots of clones with allele-specific deletions of IG^{CGI} and IG^{TRE}.

(legend continued on next page)

Please cite this article in press as: Aronson et al., A bipartite element with allele-specific functions safeguards DNA methylation imprints at the *Dlk1-Dio3* locus, Developmental Cell (2021), https://doi.org/10.1016/j.devcel.2021.10.004

(Quenneville et al., 2011; Luo et al., 2016; Riso et al., 2016; Shi et al., 2019) (Figures 1A and 1B), and components of chromatin-modifying complexes, such as PRC2 (Figure S1A). In contrast, the 1 kb of the IG-DMR closest to the *Gtl2* gene is associated with an open chromatin state enriched for the activating H3K27ac mark, nascent bidirectional transcription, the binding of multiple pluripotency-associated TFs, and general transcription regulators, consistent with a transcriptional regulatory element (TRE) function (Danko et al., 2015) (Figure S1A). These data suggest that the IG-DMR may consist of two distinct regulatory elements, which we will refer to as IG^{CGI} and IG^{TRE}.

To functionally interrogate potentially distinct roles of the IG^{CGI} and IG^{TRE} in regulating *Dlk1-Dio3*, we deleted each of these elements in iPSCs harboring a previously described allele-specific *Dlk1* reporter system (Swanzey and Stadtfeld, 2016). This transgenic system, in which maternal and paternal *Dlk1* alleles are transcriptionally linked to distinct fluorescent reporters (mVenus and tdTomato, respectively) (Figure 1C), has been shown to accurately capture the allele-specific expression of *Dlk1*, thereby reflecting the imprinting status of the entire *Dlk1-Dio3* locus (Swanzey and Stadtfeld, 2016). Since undifferentiated iPSCs do not express appreciable levels of *Dlk1*, we optimized our flow cytometry analysis approach by combining retinoic acid (RA)-induced differentiation with antibody staining against the neuroectodermal marker CD24a and gating on $CD24a^+$ cells (Semrau et al., 2017) (Figure S1B). This strategy allowed us to reliably identify instances of LOI that lead either to bi-allelic expression (LOI-BiDlk1) or complete silencing (LOI-Dlk1Loss) of *Dlk1*. Reporter iPSCs were transiently transfected with plasmids expressing Cas9 and pairs of guide RNAs (gRNAs) targeting the 5′- and 3′-ends of either IG^{CGI} and IG^{TRE} (Figure 1D; Tables S1 and S2). Strikingly, although targeting of the IG^{CGI} resulted in an increased proportion of cells that lost *Dlk1* expression (LOI-Dlk1Loss), targeting of the IG^{TRE} led to bi-allelic expression of *Dlk1* (LOI-BiDlk1) (Figure 1E). Genotyping of clonal lines obtained by single-cell sorting confirmed mono- or bi-allelic deletion of the targeted regions in cells with LOI phenotypes, whereas clones with MOI had mono-allelic deletions or unedited genomes (Figures 1F and S1C; Table S1). This established LOI-Dlk1Loss as the predominant LOI phenotype in IG^{CGI}-targeted clones and LOI-BiDlk1 in IG^{TRE}-targeted clones (Figure 1G). These phenotypes were independently validated in the context of directed differentiation toward motor neurons (Wichterle et al., 2002; Novitch et al., 2001) (Figures S1D and S1E). Quantitative PCR confirmed the *Dlk1* expression changes observed with flow cytometry and showed an inverse expression pattern between *Dlk1* and the maternally expressed lncRNA *Gtl2* (Figure 1H; Table S1). Bisulfite sequencing of ΔIG^{CGI} and ΔIG^{TRE} clones showed that both the IG-DMR itself and the Gtl2 DMR had completely lost methylation upon deletion of IG^{CGI}, whereas both control elements were fully methylated upon elimination of IG^{TRE} (Figure 1I). We observed the same imprinting phenotypes upon deletion of IG^{CGI} and IG^{TRE} in ESCs carrying the allele-specific reporter systems (Figures S1F–S1I). Taken together, these data show that the IG-DMR consists of two distinct regulatory elements with essential—but antagonistic—roles in imprinting maintenance in pluripotent cells. Deletion of these elements is sufficient to induce pronounced and specific epigenetic and transcriptional changes throughout the locus and induce either bi-maternal or bi-paternal LOI.

IG^{CGI} and IG^{TRE} are allele-specific regulators of imprinted DNA methylation and gene expression at *Dlk1-Dio3*

Next, we sought to establish the allelic specificity of IG^{CGI} and IG^{TRE}. To that end, we generated iPSCs carrying the aforementioned allele-specific *Dlk1* reporter system in a hybrid JF1/B6 F1 background (Figure 2A; Table S2). The JF1 strain carries several SNPs in the IG-DMR compared with the B6 genetic background (Koide et al., 1998) and ESCs from this strain maintain normal imprinting upon culture (Lee et al., 2018). By using gRNAs designed to target sequences with strain-specific SNPs within the first 3 base pairs downstream of the PAM sequence, we performed allele-specific CRISPR-Cas9 deletion of the IG^{CGI} and IG^{TRE} regions (Figure S2A; Tables S1 and S2). Derivation and analysis of individual clones by flow cytometry demonstrated that deletion of the paternal IG^{CGI} (ΔPat^{CGI}) was responsible for the Dlk1Loss phenotype, whereas the BiDlk1 phenotype was induced by maternal IG^{TRE} (ΔMat^{TRE}) deletion (Figures 2B and S2B). Genotyping confirmed allele-specific deletions (Figures S2C–S2F; Table S1). Although deletion of Mat^{CGI} did not result in a phenotype, some clones (10 out of 56) from the ΔPat^{TRE} targeting did result in the same BiDlk1 phenotype observed upon targeting the maternal allele. However, investigation of these clones revealed indels on the maternal allele (data not shown), indicating allelic promiscuity of Cas9 (Capon et al., 2017), supporting that ΔPat^{TRE} does not result in LOI.

Quantitative PCR analysis and subsequent sequencing of clonal amplicons confirmed the expected reciprocal effects of allele-specific Pat^{CGI} and Mat^{TRE} deletions on *Dlk1* and *Gtl2* expression, whereas knockout of the allelic counterparts resulted in no such changes (Figures 2C, 2D, and S2G; Table S1). Consistent with these findings and our results obtained via non-allele-specific genetic engineering (Figure 1I), CpGs within the IG-DMR and Gtl2 DMR were unmethylated upon paternal IG^{CGI} removal (indicating loss of the paternal imprinting mark) and hypermethylated upon maternal IG^{TRE} removal (indicating aberrant establishment of an imprinting mark on the maternal allele), whereas control cells exhibited DNA methylation levels

(C) Allele-specific *Gtl2* and *Dlk1* expression levels in RA-differentiated clones (n = 2 clones). Statistics with two-tailed unpaired Student's t test.
(D) A heterozygous SNP (arrow) in the *Gtl2* qRT-PCR amplicon allows for evaluation of allele-specific expression.
(E) Average percentage of DNA methylation in iPSCs at the IG-DMR and the Gtl2 DMR as assessed by pyrosequencing; "region 1" ($IG\text{-}DMR^{CGI}$), "region 2" ($IG\text{-}DMR^{TRE}$), and "region 3" (Gtl2 DMR). n = 2 each for clones with maternal IG^{TRE} deletion and paternal IG^{CGI} deletion. Significance with two-tailed paired Student's t test.
(F) Schematic of DNA methylation and gene expression changes upon allele-specific deletion of either IG^{CGI} or IG^{TRE}.
(G) Allele-specific 4C-seq with IG-DMR as viewpoint. Statistics for IG-DMR interaction (Mat versus Pat) with *Gtl2* and *Dlk1* are shown at chr12:109540996-109568650 (FDR = $2.3E^{-64}$ for MOI and 0.760 for ΔPat^{CGI}) and chr12:109453455-109463336 (FDR = 0.015 for MOI and 0.760 for ΔPat^{CGI}), respectively. For all panels: asterisks indicate significance: *p ≤ 0.05, **p ≤ 0.01, ***p ≤ 0.001, ****p ≤ 0.0001. n.s, not significant. Error bars represent ± SEM. See statistics summarized in Table S4.

Please cite this article in press as: Aronson et al., A bipartite element with allele-specific functions safeguards DNA methylation imprints at the *Dlk1-Dio3* locus, Developmental Cell (2021), https://doi.org/10.1016/j.devcel.2021.10.004

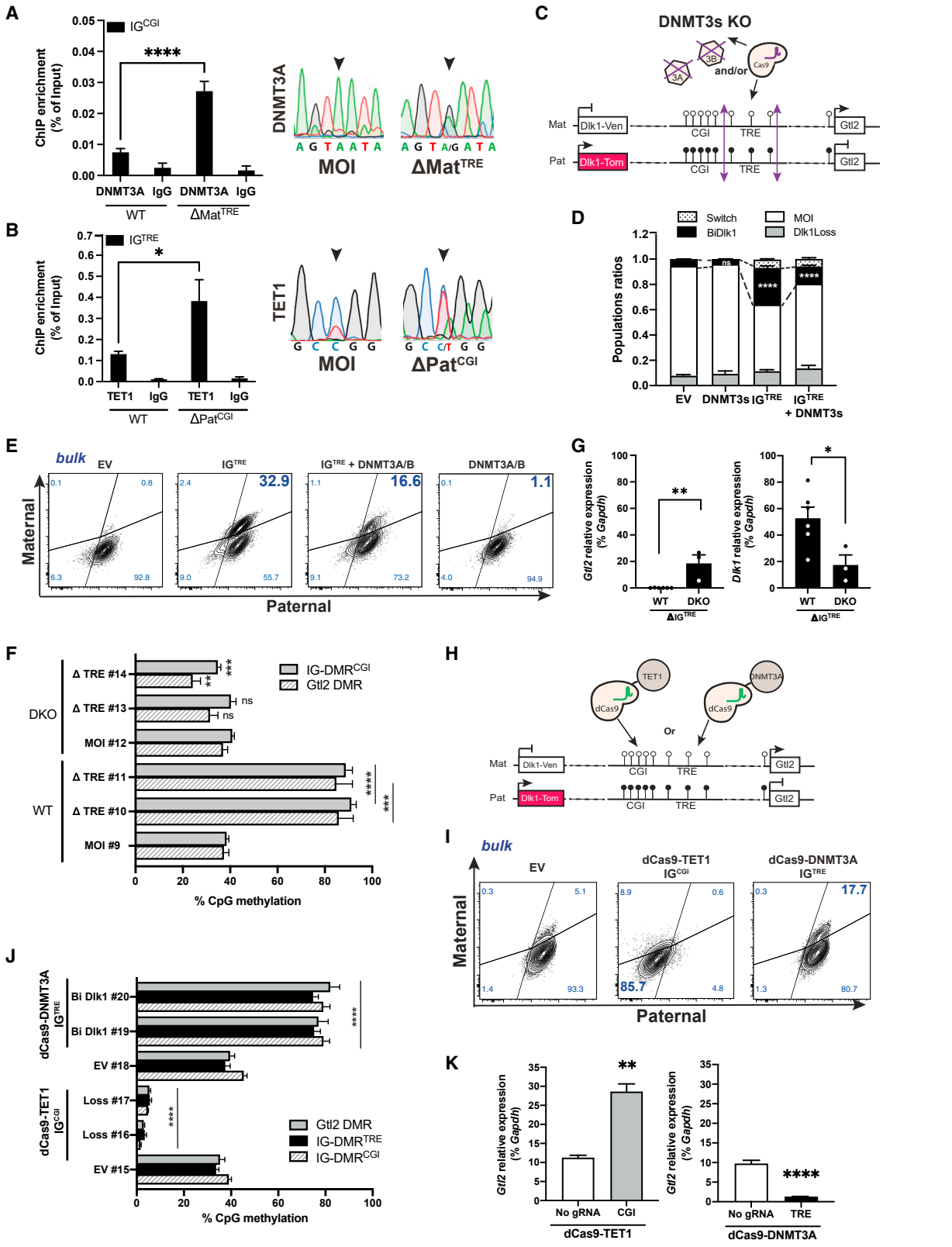

Figure 3. Allele-specific prevention of DNA methyltransferase and TET protein function by the IG-DMR

(A) Increased DNMT3A occupancy of the IG^{CGI} upon maternal IG^{TRE} deletion (left) due to bi-allelic binding (right) as measured by ChIP-qPCR and sequencing of PCR products.

(legend continued on next page)

Please cite this article in press as: Aronson et al., A bipartite element with allele-specific functions safeguards DNA methylation imprints at the *Dlk1-Dio3* locus, Developmental Cell (2021), https://doi.org/10.1016/j.devcel.2021.10.004

typical for epigenetically intact naive pluripotent cells (Carey et al., 2011; Stadtfeld et al., 2010) (Figure 2E; Table S3).

To investigate whether additional chromatin changes occur in the locus, we performed allele-specific chromatin immunoprecipitation (as-ChIP) for the active histone mark H3K27ac, followed by Sanger sequencing. Although MOI cells strongly enriched for H3K27ac only on the maternal IG-DMR and Gtl2 DMR, ΔPat^{CGI} clones exhibited bi-allelic H3K27ac, and ΔMat^{TRE} clones lost H3K27ac almost entirely (Figure S2H; Table S1). Collectively, our results demonstrate that the unmethylated IG^{TRE} is associated with *Gtl2* expression and an active chromatin state on the maternal allele, whereas the methylated IG^{CGI} correlates with *Gtl2* repression and an inactive chromatin state on the paternal allele (Figure 2F).

We also asked whether the observed epigenetic and transcriptional changes were accompanied by 3D chromatin reorganization around the locus, by using allele-specific 4C-seq. In agreement with recent reports (Llères et al., 2019), we found that the long-range chromatin contacts around the IG-DMR differ between the maternal and paternal alleles. Specifically, the maternal unmethylated IG-DMR interacts at high frequency with *Gtl2*, whereas these interactions are significantly weaker on the paternal allele (Figure 2G). In addition, we found a subtle interaction of the maternal IG-DMR with *Dlk1* that, although statistically significant, is marginal and unlikely to be representative of consistent close proximity between these loci (Figure 2G). Deletion of the paternal IG^{CGI} perturbed this allele-specific topology and induced a maternal-like conformation on both alleles (Figure 2G; Table S1). On the other hand, deletion of the maternal IG^{TRE} induced a significant overall decrease of interactivity resembling a bi-paternal topology (Figure S2I). These results suggest that DNA methylation of IG^{CGI} might prevent the physical interaction of the IG-DMR with its target genes and that IG^{TRE} is essential for the maintenance of these long-range chromatin contacts. Taken together, our observations show that the paternal IG^{CGI} and maternal IG^{TRE} have distinct regulatory functions that are required to maintain the respective alleles in epigenetic and conformational states consistent with MOI at *Dlk1-Dio3*.

The bipartite nature of the IG-DMR results in allele-specific suppression of the DNA methylation machinery

De novo DNA methyltransferases and TET dioxygenases operate at ICRs to establish and erase methylation in germ cells during development (Li and Sasaki, 2011; Bartolomei and Ferguson-Smith, 2011; Plasschaert and Bartolomei, 2014; SanMiguel and Bartolomei, 2018). The allele-specific DNA methylation changes that we observed upon IG^{TRE} and IG^{CGI} deletion (Figure 2E) raised the possibility that these enzymes might also be involved in the induction of the distinct LOI phenotypes. In agreement with this, allele-specific chromatin immunoprecipitation (ChIP) experiments documented that DNMT3A, which normally only binds to the paternal allele of the IG-DMR, acquired bi-allelic binding upon deletion of the IG^{TRE} (Figures 3A and S3A). Similarly, we found TET1 to be bound to both alleles of the IG-DMR only upon IG^{CGI} deletion (Figures 3B and S3A). To directly assess the importance of *de novo* DNA methylation for LOI, we deleted IG^{TRE} in parallel to the gene loci encoding DNMT3A and DNMT3B (*Dnmt3a/b*) in *Dlk1* reporter iPSCs using Cas9 technology (Figure 3C; Table S1). Subsequent differentiation and FACS analysis of bulk populations showed a significant amelioration of the LOI-BiDlk1 phenotype and an increased proportion of cells that retained MOI (Figures 3D and 3E). Genotyping of targeted regions and surveyor assays in bulk populations confirmed the respective deletions and indels by CRISPR-Cas9 and showed amplicons of equal strength, demonstrating similar degrees of targeting efficiency across experimental conditions (Figure S3B; Table S1). To confirm these observations at the single-cell level, we derived and validated clonal ΔIG^{TRE} cell lines from previously characterized DNMT3A/B knockout (DKO) (Lei et al., 1996; Okano et al., 1999) and parental control ESCs. In contrast to wild-type (WT) cells, DKO ESCs lacking the IG^{TRE} did not acquire DNA hypermethylation at either IG-DMR or Gtl2 DMR before (Figure 3F) or after (Figure S3C) differentiation. This is consistent with the notion that IG^{TRE} antagonizes the activity of canonical *de novo* methyltransferases on the maternal allele, as suggested by ChIP. Nevertheless, *Gtl2* expression in ESCs without IG^{TRE} remained low even in the absence of DNMT3A/B (Figure S3D). However, upon RA differentiation, DNMT3A/B KO ESCs—but not WT ESCs lacking the IG^{TRE}—were able to upregulate *Gtl2*, which was associated with significantly reduced levels of *Dlk1* expression (Figure 3G). Together, these observations suggest that misdirected DNMT3A/B activity contributes to the LOI phenotype observed upon loss of the IG^{TRE}. Of note, the ablation of DNMT3A/B in reporter iPSCs without simultaneous removal of IG^{TRE} showed no effects on imprinting stability. This is consistent with prior reports indicating that these two enzymes are not required for MOI at *Dlk1-Dio3* in mouse embryos with an intact IG-DMR (Hirasawa et al., 2008).

(B) Increased TET1 occupancy of the IG^{TRE} upon paternal IG^{CGI} deletion (left) due to bi-allelic binding (right) as measured by ChIP-qPCR and sequencing of PCR products. n = 2 clones for (A) and (B).
(C) Schematic of combined IG-DMR editing and *Dnmt3a/b* deletion.
(D) Ratios of phenotypic populations in pooled populations upon targeting Dnmt3a/b and IG^{TRE} alone or in combination n = 6 experiments. Statistical significance compared with EV (dashed line) with two-tailed unpaired Student's t test.
(E) Representative bulk populations FACS plots upon indicated deletions.
(F) Average percentage of DNA methylation in RA-differentiated clones at IG-DMR and Gtl2 DMR as assessed by pyrosequencing; "region 1" ($IG\text{-}DMR^{CGI}$), "region 2" ($IG\text{-}DMR^{TRE}$), and "region 3" (Gtl2 DMR).
(G) *Dlk1* and *Gtl2* expression relative to *Gapdh* in six WT and three DNMT3A/B knockout (DKO) RA-differentiated IG^{TRE} clones.
(H and I) (H) Strategy of targeting dCas9-TET1 to the IG^{CGI} or dCas9-DNMT3A to the IG^{TRE} and (I) representative bulk population FACS plots after implementation.
(J) DNA methylation in iPSCs after indicated dCas9 targeting; "region 1" ($IG\text{-}DMR^{CGI}$), "region 2" ($IG\text{-}DMR^{TRE}$), and "region 3" (Gtl2 DMR). Statistical significance with two-tailed paired Student's t test relative to the respective EV clone (see also Tables S2, S3, and S4).
(K) *Gtl2* RNA expression levels in dCas9-TET1 and dCas9-DNMT3A iPSCs. Statistical significance with two-tailed unpaired Student's t test. For all panels: asterisks indicate significance: $^{*}p \leq 0.05$, $^{**}p \leq 0.01$, $^{***}p \leq 0.001$, $^{****}p \leq 0.0001$. n.s, not significant. Error bars represent ± SEM. See statistics summarized in Table S4.

Please cite this article in press as: Aronson et al., A bipartite element with allele-specific functions safeguards DNA methylation imprints at the *Dlk1-Dio3* locus, Developmental Cell (2021), https://doi.org/10.1016/j.devcel.2021.10.004

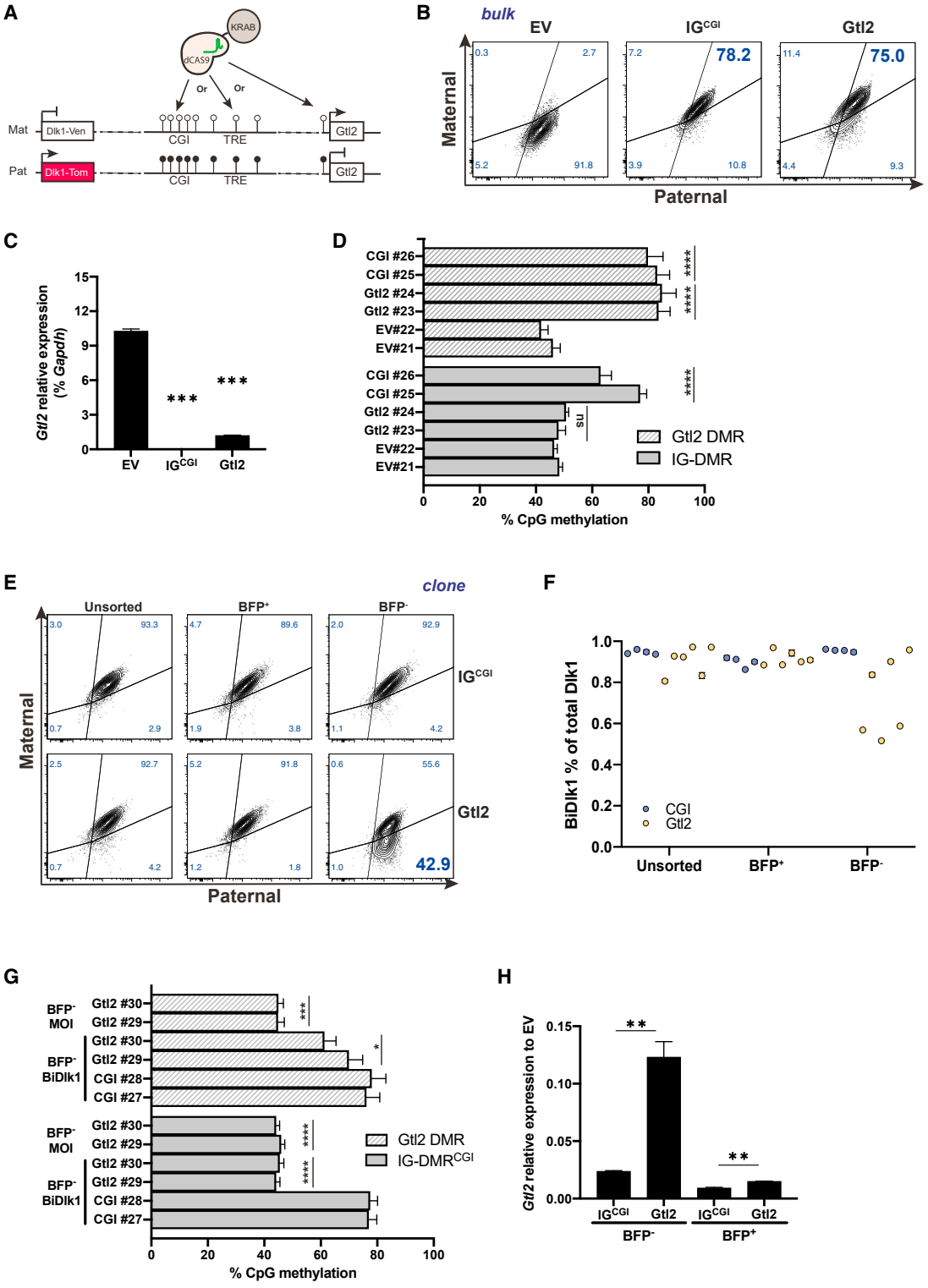

Figure 4. IG-DMR methylation status dictates *Dlk1-Dio3* imprinting stability

(A) Strategy to element-specific targeting of dCas9-BFP-KRAB.

(B) Representative FACS plots showing dominant LOI-BiDlk1 populations after bi-allelic KRAB targeting to either IG^{CGI} or *Gtl2* promoter (see also Figure S4A).

(C) qRT-PCR analysis of *Gtl2* expression in indicated cells. Statistical significance was calculated by two-tailed unpaired Student's t test.

(D) Average percentage of methylated CpGs at IG-DMR and Gtl2 DMR as determined by bisulfite sequencing analysis. Note that targeting dCas9-BFP-KRAB to the Gtl2 DMR does not result in hypermethylation at the IG-DMR. Statistical analysis by comparison with the EV controls using two-tailed paired Student's t test.

(legend continued on next page)

Please cite this article in press as: Aronson et al., A bipartite element with allele-specific functions safeguards DNA methylation imprints at the *Dlk1-Dio3* locus, Developmental Cell (2021), https://doi.org/10.1016/j.devcel.2021.10.004

Similar to our observations with DNMT3A/B and the IG^{TRE}, flow cytometric analysis of iPSCs after simultaneous deletion of the IG^{CGI} and the genes encoding all TET proteins (*Tet1, Tet2*, and *Tet3*) (Dawlaty et al., 2014) suggested amelioration of the LOI-Dlk1 phenotype (Figures S3E–S3H). However, analysis of clones derived from either TET1/2/3-deficient or WT ESCs several weeks after IG^{CGI} deletion showed loss of DNA methylation at the IG-DMR in almost all cell lines (Figure S3I) and comparable *Dlk1/Gtl2* expression levels (Figure S3J), suggesting that LOI upon IG^{CGI} deletion is inevitable even in the absence of TET enzymes, possibly by passive DNA demethylation.

Together, the experiments further highlight the essential roles of IG^{TRE} and IG^{CGI} in preventing *de novo* DNA methylation or demethylation, respectively, and thus maintaining *Dlk1-Dio3* imprinting.

Forced gain or loss of DNA methylation at the IG-DMR is sufficient to induce LOI

The results described earlier demonstrate that the protection of allele-specific DNA methylation states by the IG^{CGI} and IG^{TRE} are important to maintain imprinting at *Dlk1-Dio3*. Therefore, we asked whether local DNA methylation changes at either of these respective elements could phenocopy the effect of the respective genetic deletions on imprint stability. We generated *Dlk1* reporter iPSCs that express a catalytically deactivated Cas9 (dCas9) fused to the catalytic domain of either TET1 or DNMT3A (Tables S1 and S2) (Xu et al., 2016; Choudhury et al., 2016; Morita et al., 2016; Verma et al., 2018). We then stably expressed multiplexed gRNAs, targeting either three ZFP57 binding sites within the IG^{CGI} or the sites of nascent transcription of the IG^{TRE} (Figure 3H; Table S1). We observed that targeting of dCas9-TET1 to the IG^{CGI} resulted in conversion of almost all cells to the LOI-Dlk1Loss phenotype (Figure 3I), recapitulating our observations upon deletion of the Pat^{CGI} (Figure 2B). This phenotype was accompanied by loss of DNA methylation on both IG-DMR and Gtl2 DMR along with *Gtl2* upregulation (Figures 3J and 3K; Table S1). On the other hand, targeting of dCas9-DNMT3A to the IG^{TRE} induced a LOI-BiDlk1 population with respective hypermethylation and loss of *Gtl2* expression (Figures 3H–3K). Taken together, these experiments demonstrate that local changes in DNA methylation at the IG^{CGI} and IG^{TRE} are sufficient to affect the methylation status at the distal Gtl2 DMR and perturb imprinted gene expression.

DMR-specific targeting of CRISPRi results in either transient or irreversible LOI

So far, our results have shown that allele-specific genetic or epigenetic manipulation of the specific elements within the IG-DMR induces LOI phenotypes that correlate with methylation and transcriptional changes at the *Gtl2*. To test whether the regulatory function of the IG-DMR can be overridden by direct silencing of *Gtl2*, we generated stable reporter iPSCs expressing the transcriptional repressor dCas9-BFP-KRAB (CRISPRi) and gRNAs that target either the IG^{CGI}, the IG^{TRE}, or the Gtl2 DMR (Figure 4A; Table S1). Of note, the KRAB domain used in our experiments was shown to mediate stable *de novo* DNA methylation in early embryonic cells (Quenneville et al., 2012; Ying et al., 2015). Consistent with dCas9-mediated epigenetic editing of the IG-DMR (Figures 3H–3K), targeting of CRISPRi to either the IG^{CGI} or IG^{TRE} resulted in hypermethylation of the IG-DMR and Gtl2 DMR, as well as *Gtl2* repression (Figures 4B–4D, S4A, and S4B). Targeting of the Gtl2 DMR similarly triggered a high degree of LOI-BiDlk1, but in contrast to IG-DMR targeting, it only induced local Gtl2 DMR hypermethylation without affecting the methylation status of the IG-DMR (Figure 4D). This demonstrates that targeted repression of *Gtl2* is sufficient to activate maternal *Dlk1* without acquisition of DNA methylation at the IG-DMR. To test whether the absence of IG-DMR hypermethylation might affect the stability of this LOI phenotype, we made use of the observation that our lentiviral CRISPRi, without continuous resorting or reselection, is silenced over time in PSCs. We established BFP^{+} and BFP^{-} subclones from originally BFP^{+} (i.e., dCas9-BFP-KRAB-expressing) cells, followed by extensive passaging, allowing for potential reversal of epigenetic effects after dCas9-KRAB (Mandegar et al., 2016). This was done in cells where CRISPRi was targeted either to the IG^{CGI} or to the Gtl2 DMR. FACS analysis showed that all CGI-targeted clones retained their LOI-BiDlk1 phenotype and hypermethylation of both IG-DMR and Gtl2 DMR, independent of their BFP expression status (Figures 4E and 4F). This demonstrates that the change in imprinting status was irreversible. In contrast, three out of six *Gtl2*-targeted BFP^{-} clones partially reverted to MOI (Figures 4E, 4F, and S4C). This partial rescue was not seen in clones that retained CRISPRi expression (BFP^{+}). Bisulfite sequencing of the MOI population of partially rescued clones showed reestablishment of normal methylation levels (~50%) at the *Gtl2* promoter. Interestingly, the remaining BiDlk1 population of rescued clones showed intermediate levels of methylation that were ~10% reduced compared with clones still expressing CRISPRi, suggesting an ongoing DNA demethylation that could reach MOI levels upon further passaging (Figure 4G). Furthermore, qPCR analysis confirmed that *Gtl2* expression was significantly increased in rescued *Gtl2*-targeted clones compared with CGI-targeted clones that had lost CRISPRi expression (Figure 4H; Table S1). These results suggest that although modulating the activity or methylation of the *Gtl2* promoter can transiently alter gene expression at *Dlk1-Dio3*, the DNA methylation status of the IG-DMR is the determining factor for long-term imprinting stability of this cluster.

DISCUSSION

In this study, we combine genetic engineering with targeted epigenetic editing in mouse PSCs to dissect the regulatory

(E) FACS plots of dCas9-BFP-KRAB CGI-targeted clone and a rescued *Gtl2*-targeted clone at passage 15 (p15).
(F) Percentage of the LOI-BiDlk1 population in n = 4 dCas9-BFP-KRAB CGI-targeted clones and n = 6 Gtl2-targeted clones at p15.
(G) Bisulfite sequencing analysis in iPSCs of MOI and BiDlk1 populations of two rescued dCas9-BFP-KRAB-targeted clones; "region 1" ($IG\text{-}DMR^{CGI}$) and "region 3" (Gtl2 DMR). Statistical significance with two-tailed paired Student's t test using CGI clones #27 and #28 as controls (see Table S2).
(H) qRT-PCR analysis of *Gtl2* expression in the BFP^{-} populations of Gtl2-targeted and IG^{CGI}-targeted clones. Statistical analysis by comparison within each BFP^{-} or BFP^{+} population and normalized to EV using two-tailed paired Student's t test. For all panels: asterisks indicate significance: *p ≤ 0.05, **p ≤ 0.01, ***p ≤ 0.001, ****p ≤ 0.0001. n.s, not significant. Error bars represent ± SEM. See statistics summarized in Table S4.

Please cite this article in press as: Aronson et al., A bipartite element with allele-specific functions safeguards DNA methylation imprints at the *Dlk1-Dio3* locus, Developmental Cell (2021), https://doi.org/10.1016/j.devcel.2021.10.004

mechanisms that protect imprint stability at *Dlk1-Dio3*, a gene cluster essential for mammalian development. Our findings extend prior studies that have identified the IG-DMR as the critical control element of *Dlk1-Dio3* (Lin et al., 2003; Nowak et al., 2011; Kota et al., 2014; Luo et al., 2016; Wang et al., 2017; Saito et al., 2018) and reconcile previously divergent *in vivo* phenotypes upon knockout of different parts of the IG-DMR (Hara et al., 2019; Lin et al., 2003; Saito et al., 2018). More importantly, our study provides insights into the IG-DMR structure and mechanisms of action that can be exploited to modulate *Dlk1-Dio3* imprinting status in a predictable fashion.

By allele-specific CRISPR knockout experiments, we revealed that the IG-DMR is a bipartite element, composed of a repressive element (IG^{CGI}) that functions on the paternal allele and an activating element (IG^{TRE}) on the maternal allele, both of which are necessary to maintain allele-specific gene expression over distance (Figure S4D). Deletion of each element from the respective allele results in either bi-paternal or bi-maternal LOI, whereas reciprocal deletions show normal imprinting. Furthermore, we provide evidence that the two elements of IG-DMR independently safeguard the imprinted DNA methylation state of *Dlk1-Dio3* by restricting the competing *de novo* DNA methylation and demethylation activities on the locus in an allele-specific manner. All these features document that the IG-DMR is distinct from other previously described composite ICRs, which serve as methylation-sensitive insulator boundaries, as in the case of *Rasgrf1* and *Snrpn* (Yoon et al., 2005; Bartolomei, 2009; Rabinovitz et al., 2012; Hsiao et al., 2019). Intriguingly, some of the molecular characteristics of the IG-DMR resemble the features of so-called orphan CGIs, which are distal to promoters and are characterized by active enhancer marks, such as H3K27ac, topological interactions with nearby target genes, and overlapping ZFP57 and MLL1 consensus motifs (Quenneville et al., 2011; Anvar et al., 2016; Bae et al., 2016; Bina, 2017; Bell and Vertino, 2017; Mendizabal and Yi, 2016). Importantly, similar to the IG-DMR, the activity of orphan CGIs is controlled by DNA methylation (Illingworth et al., 2010). Orphan CGIs were also recently shown to mediate physical and functional communication between poised enhancers and target developmental genes (Pachano et al., 2021). Future experiments will be required to identify functional commonalities between IG-DMR and orphan CGI enhancers.

It has previously been suggested that the IG-DMR functions as an enhancer for *Gtl2* expression (Lin et al., 2003; Kota et al., 2014; Das et al., 2015; Luo et al., 2016; Wang et al., 2017). Consistent with these studies, we found that deletion of the IG-DMR, and specifically the maternal unmethylated IG^{TRE}, resulted in transcriptional silencing of *Gtl2* in PSCs and also in DNA hypermethylation of both IG-DMR and Gtl2 DMR. Deletion of IG^{TRE} in the absence of DNA methyltransferase activity allowed us to functionally uncouple these molecular effects. This supported a dual function of the IG^{TRE}, both as a transcriptional enhancer of *Gtl2* in PSCs and, more importantly, as a guardian of the unmethylated status of the maternal Gtl2 DMR, thereby maintaining proper imprinting of the locus. The activation of *Gtl2* expression upon differentiation of DNMT3A/B-deficient ESCs even in the absence of the IG^{TRE} suggests the presence of additional cell-type-specific enhancers and/or of *trans*-acting factors that can act directly upon the *Gtl2* promoter in differentiated cells when the latter is unmethylated. Whether this non-canonical enhancer function is present in other ICRs or developmental loci remains to be shown. The factors and mechanisms that counteract DNA methyltransferase activity on IG^{TRE} and the distal Gtl2 DMR remain elusive. Our CRISPRi experiments support that the active chromatin and transcriptional status of IG^{TRE} is necessary for protecting the maternal allele from *de novo* DNA methylation, both locally and on the Gtl2 DMR, potentially through looping (Figure S4D). Indeed, active histone marks (Rose and Klose, 2014), as well as binding of TF or the activating complex CBP/p300, have been shown to protect CpG sites from DNMT3A/B activity (Gebhard et al., 2010; Lienert et al., 2011; Straussman et al., 2009; Zhang et al., 2017). Similarly, the nascent non-coding transcripts of the locus (enhancer RNA and/or Gtl2 non-coding RNA) may also play a protective role, as has been previously suggested (Kota et al., 2014), by either interacting with PRC2 (Das et al., 2015) or DNMT3A/B and DNMT1 (Zhao et al., 2016; Morlando and Fatica, 2018). Finally, recent studies demonstrated that a class of TF, including key pluripotency regulators such as SOX2 and KLF4, which bind on IG^{TRE}, can directly prevent DNA methylation or even induce demethylation of their target sites (Vanzan et al., 2021). Further investigation will be required to dissect the relative contribution of each of these factors in MOI at *Dlk1-Dio3*.

In sharp contrast to IG^{TRE}, which blocks *de novo* DNA methylation on the maternal allele, our experiments showed that IG^{CGI} is essential for preventing both TET-dependent and independent DNA demethylation of the paternal DMRs. Several *trans*-acting factors could mediate this function (Figure S4D). A potential candidate is the KRAB domain containing zinc-finger ZFP57, which has been shown to bind to the methylated IG-DMR in the region of the IG^{CGI} (Riso et al., 2016; Luo et al., 2016; Strogantsev et al., 2015; Shi et al., 2019) and maintains closed chromatin by recruiting repressive complexes, such as DNA and H3K9 methyltransferases (Quenneville et al., 2011; Riso et al., 2016). Moreover, knockdown of *Zfp57* has been shown to cause accumulation of 5-hydroxymethylcytosine (5hmC) at the IG-DMR (Coluccio et al., 2018), which suggests that this protein is involved in preventing TET binding and activity, as well as passive DNA demethylation on the paternal IG-DMR.

To further dissect the regulatory logic of the *Dlk1-Dio3 locus*, we harnessed the power of dCas9 epigenetic editing (Hsu et al., 2014). These experiments revealed a hierarchical and unidirectional regulation between IG-DMR and Gtl2 DMR that is substantiated by the following key observations. First, although any targeted modulation of the IG-DMR (either by dCas9-TET1, dCas9-DNMT3A, or CRISPRi) resulted in methylation changes on both DMRs, targeting of the Gtl2 DMR affected only local DNA methylation without any effects on IG-DMR, suggesting a "one-way" communication. In addition, although targeting of the Gtl2 DMR can cause LOI, normal imprinting can be restored by the IG-DMR, suggesting that this element controls long-term imprinting stability. These observations are consistent with the observation that the *Gtl2* promoter acquires allele-specific DNA methylation during embryonic development to match the status of the IG-DMR (Sato et al., 2011). Dissecting the molecular mechanisms (e.g., physical proximity or spreading) underlying this regulatory hierarchy and their degree of conservation among cell

types (Alexander and Garcia-Garcia, 2019) and species would be interesting areas for future investigation, in particular, in the context of imprinting disorders.

In conclusion, our study refined the mechanistic understanding of the regulatory logic that safeguards imprinting stability at *Dlk1-Dio3* and revealed ways to perturb this logic in a rationale and predictable manner. Although previously reported *in vivo* phenotypes are consistent with a bi-partite nature of the IG-DMR, additional work will be required to dissect the precise function of IG^{CGI} and IG^{TRE} during establishment and maintenance of *Dlk1-Dio3* imprinting in the organism. We envision that the molecular principles operational at the IG-DMR may serve as paradigms to better understand the epigenetic regulation of other developmental gene loci.

Limitations of the study

Although this work provides a detailed investigation of the molecular function of the IG-DMR in maintaining genomic imprinting in mouse pluripotent cells, additional work will be required to confirm the bipartite nature of this control element in other cell types and during the initial establishment of *Dlk1-Dio3* imprinting in male germ cells *in vivo*. In addition, the precise molecular mechanisms of LOI downstream of inactivation of IG^{CGI} and IG^{TRE}—such as the involvement of additional protein and non-protein factors and their relationship to DNMT3A/B and TET proteins—remain to be elucidated.

STAR★METHODS

Detailed methods are provided in the online version of this paper and include the following:

- KEY RESOURCES TABLE
- RESOURCE AVAILABILITY
  - Lead contact
  - Materials availability
  - Data and code availability
- EXPERIMENTAL MODELS AND SUBJECT DETAILS
  - Cell lines
  - Animals
- METHOD DETAILS
  - ESC and iPSC cell culture
  - Generating allele-specific iPSC *Dlk1*-reporter in hybrid maternal JF1/paternal B6 background
  - PSC with CRISPR/Cas9 mediated deletions
  - Cloning of multiple gRNA expression vectors for dCas9 expressing iPSC's
  - Cloning of dCas9 plasmids
  - Lentiviral production and infection
  - Generation of stable dCas9 expressing cell lines
  - Retinoic acid differentiation assays
  - Flow cytometry
  - qPCR
  - Bisulfite conversion and pyrosequencing
  - ChIP-qPCR
  - 4C-seq
  - Motor neuron differentiation assays
  - Immunocytochemistry
- QUANTIFICATION AND STATISTICAL ANALYSIS
  - Analysis of 4C-seq data
  - Statistical analysis

SUPPLEMENTAL INFORMATION

Supplemental information can be found online at https://doi.org/10.1016/j.devcel.2021.10.004.

ACKNOWLEDGMENTS

We are grateful to A. Melnick, R. Chaligne, and the members of the Apostolou, Tsirigos, and Stadtfeld laboratories for critical reading of the manuscript, to N. Ben Chetrit for advice on microscopy experiments, and to D. Huangfu and L. Dow for sharing CRISPR–Cas9 vectors. B.E.A. is supported by the National Health Institutes, the National Cancer Institute (NCI) grant T32 CA203702; L.S. is supported by the Lady TATA Memorial Fund and the Lymphoma Research Foundation; A.T. is supported by the NCI (P01CA229086 and R01CA252239); B.P.-W. is supported by the NICHD with a T32 (T32HD060600) and an F30 (F30HD097926), as well as by a Medical Scientist Training Program grant from the NIGMS under award number T32GM007739 to the Weill Cornell/Rockefeller/Sloan Kettering Tri-Institutional MD-PhD Program; M.S. is supported by grants from the NIH (R01GM121994) and the Tri-Institutional Stem Cell Initiative by the Starr Foundation (Tri-SCI); and E.A. is supported by the Edward Mallinckrodt Jr. Foundation, the NIH (DP2DA043813 and R01GM138635), and Tri-SCI.

AUTHOR CONTRIBUTIONS

Conceptualization, B.E.A., L.S., M.S., and E.A.; methodology, B.E.A., L.S., E.S., M.M.D., M.S., and E.A.; formal analysis, A.K. and A.P.; investigation, B.E.A., L.S., V.S., A.S., A.A., I.C., J.L., B.P.-W. and R.A.G., .; writing – original draft, B.E.A., L.S., M.S., and E.A.; supervision, H.W., T.V., M.S., and E.A.

DECLARATION OF INTERESTS

The authors declare no competing interests.

Received: April 17, 2020
Revised: August 6, 2021
Accepted: October 4, 2021
Published: October 27, 2021

REFERENCES

Alexander, K.A., and Garcia-Garcia, M.J. (2019). Imprinted gene expression at the Dlk1-Dio3 cluster is controlled by both maternal and paternal *IG-DMRs* in a tissue-specific fashion. bioRxiv. https://doi.org/10.1101/536102.

Anvar, Z., Cammisa, M., Riso, V., Baglivo, I., Kukreja, H., Sparago, A., Girardot, M., Lad, S., De Feis, I., Cerrato, F., et al. (2016). ZFP57 recognizes multiple and closely spaced sequence motif variants to maintain repressive epigenetic marks in mouse embryonic stem cells. Nucleic Acids Res. *44*, 1118–1132.

Bae, M.G., Kim, J.Y., and Choi, J.K. (2016). Frequent hypermethylation of orphan CpG islands with enhancer activity in cancer. BMC Med. Genomics *9* (suppl 1), 38.

Bartolomei, M.S. (2009). Genomic imprinting: employing and avoiding epigenetic processes. Genes Dev. *23*, 2124–2133.

Bartolomei, M.S., and Ferguson-Smith, A.C. (2011). Mammalian genomic imprinting. Cold Spring Harb. Perspect. Biol. *3*, a002592.

Bell, J.S.K., and Vertino, P.M. (2017). Orphan CpG islands define a novel class of highly active enhancers. Epigenetics *12*, 449–464.

Bina, M. (2017). Imprinted control regions include composite DNA elements consisting of the ZFP57 binding site overlapping MLL1 morphemes. Genomics *109*, 265–273.

Capon, S.J., Baillie, G.J., Bower, N.I., Da Silva, J.A., Paterson, S., Hogan, B.M., Simons, C., and Smith, K.A. (2017). Utilising polymorphisms to achieve allele-specific genome editing in zebrafish. Biol. Open *6*, 125–131.

Carey, B.W., Markoulaki, S., Hanna, J.H., Faddah, D.A., Buganim, Y., Kim, J., Ganz, K., Steine, E.J., Cassady, J.P., Creyghton, M.P., et al. (2011). Reprogramming factor stoichiometry influences the epigenetic state and biological properties of induced pluripotent stem cells. Cell Stem Cell *9*, 588–598.

Chen, B., Gilbert, L.A., Cimini, B.A., Schnitzbauer, J., Zhang, W., Li, G.W., Park, J., Blackburn, E.H., Weissman, J.S., Qi, L.S., and Huang, B. (2013). Dynamic imaging of genomic loci in living human cells by an optimized CRISPR/Cas system. Cell *155*, 1479–1491.

Choudhury, S.R., Cui, Y., Lubecka, K., Stefanska, B., and Irudayaraj, J. (2016). CRISPR-dCas9 mediated TET1 targeting for selective DNA demethylation at BRCA1 promoter. Oncotarget *7*, 46545–46556.

Coluccio, A., Ecco, G., Duc, J., Offner, S., Turelli, P., and Trono, D. (2018). Individual retrotransposon integrants are differentially controlled by KZFP/KAP1-dependent histone methylation, DNA methylation and TET-mediated hydroxymethylation in naive embryonic stem cells. Epigenetics Chromatin *11*, 7.

Cong, L., Ran, F.A., Cox, D., Lin, S., Barretto, R., Habib, N., Hsu, P.D., Wu, X., Jiang, W., Marraffini, L.A., et al. (2013). Multiplex genome engineering using CRISPR/Cas systems. Science *339*, 819–823.

Da Rocha, S.T., Edwards, C.A., Ito, M., Ogata, T., and Ferguson-Smith, A.C. (2008). Genomic imprinting at the mammalian Dlk1-Dio3 domain. Trends Genet. *24*, 306–316.

Danko, C.G., Hyland, S.L., Core, L.J., Martins, A.L., Waters, C.T., Lee, H.W., Cheung, V.G., Kraus, W.L., Lis, J.T., and Siepel, A. (2015). Identification of active transcriptional regulatory elements from GRO-seq data. Nat. Methods *12*, 433–438.

Das, P.P., Hendrix, D.A., Apostolou, E., Buchner, A.H., Canver, M.C., Beyaz, S., Ljuboja, D., Kuintzle, R., Kim, W., Karnik, R., et al. (2015). PRC2 is required to maintain expression of the maternal Gtl2-Rian-Mirg locus by preventing de novo DNA methylation in mouse embryonic stem cells. Cell Rep. *12*, 1456–1470.

Dawlaty, M.M., Breiling, A., Le, T., Barrasa, M.I., Raddatz, G., Gao, Q., Powell, B.E., Cheng, A.W., Faull, K.F., Lyko, F., and Jaenisch, R. (2014). Loss of Tet enzymes compromises proper differentiation of embryonic stem cells. Dev. Cell *29*, 102–111.

Di Giammartino, D.C., Kloetgen, A., Polyzos, A., Liu, Y., Kim, D., Murphy, D., Abuhashem, A., Cavaliere, P., Aronson, B., Shah, V., et al. (2019). KLF4 is involved in the organization and regulation of pluripotency-associated three-dimensional enhancer networks. Nat. Cell Biol. *21*, 1179–1190.

Dow, L.E., Fisher, J., O'Rourke, K.P., Muley, A., Kastenhuber, E.R., Livshits, G., Tschaharganeh, D.F., Socci, N.D., and Lowe, S.W. (2015). Inducible in vivo genome editing with CRISPR-Cas9. Nat. Biotechnol. *33*, 390–394.

Ferguson-Smith, A.C., and Bourc'his, D. (2018). The discovery and importance of genomic imprinting. eLife *7*, e42368.

Gebhard, C., Benner, C., Ehrich, M., Schwarzfischer, L., Schilling, E., Klug, M., Dietmaier, W., Thiede, C., Holler, E., Andreesen, R., and Rehli, M. (2010). General transcription factor binding at CpG islands in normal cells correlates with resistance to de novo DNA methylation in cancer cells. Cancer Res. *70*, 1398–1407.

Gilbert, L.A., Larson, M.H., Morsut, L., Liu, Z., Brar, G.A., Torres, S.E., Stern-Ginossar, N., Brandman, O., Whitehead, E.H., Doudna, J.A., et al. (2013). CRISPR-mediated modular RNA-guided regulation of transcription in eukaryotes. Cell *154*, 442–451.

Guschin, D.Y., Waite, A.J., Katibah, G.E., Miller, J.C., Holmes, M.C., and Rebar, E.J. (2010). A rapid and general assay for monitoring endogenous gene modification. Methods Mol. Biol. *649*, 247–256.

Hara, S., Terao, M., Muramatsu, A., and Takada, S. (2019). Efficient production and transmission of CRISPR/Cas9-mediated mutant alleles at the IG-DMR via generation of mosaic mice using a modified 2CC method. Sci. Rep. *9*, 20202.

Heckl, D., Kowalczyk, M.S., Yudovich, D., Belizaire, R., Puram, R.V., Mcconkey, M.E., Thielke, A., Aster, J.C., Regev, A., and Ebert, B.L. (2014). Generation of mouse models of myeloid malignancy with combinatorial genetic lesions using CRISPR-Cas9 genome editing. Nat. Biotechnol. *32*, 941–946.

Hirasawa, R., Chiba, H., Kaneda, M., Tajima, S., Li, E., Jaenisch, R., and Sasaki, H. (2008). Maternal and zygotic Dnmt1 are necessary and sufficient for the maintenance of DNA methylation imprints during preimplantation development. Genes Dev. *22*, 1607–1616.

Hiura, H., Komiyama, J., Shirai, M., Obata, Y., Ogawa, H., and Kono, T. (2007). DNA methylation imprints on the IG-DMR of the Dlk1-Gtl2 domain in mouse male germline. FEBS Lett. *581*, 1255–1260.

Hsiao, J.S., Germain, N.D., Wilderman, A., Stoddard, C., Wojenski, L.A., Villafano, G.J., Core, L., Cotney, J., and Chamberlain, S.J. (2019). A bipartite boundary element restricts UBE3A imprinting to mature neurons. Proc. Natl. Acad. Sci. USA *116*, 2181–2186.

Hsu, P.D., Lander, E.S., and Zhang, F. (2014). Development and applications of CRISPR-Cas9 for genome engineering. Cell *157*, 1262–1278.

Illingworth, R.S., Gruenewald-Schneider, U., Webb, S., Kerr, A.R., James, K.D., Turner, D.J., Smith, C., Harrison, D.J., Andrews, R., and Bird, A.P. (2010). Orphan CpG islands identify numerous conserved promoters in the mammalian genome. PLoS Genet. *6*, e1001134.

Jelinic, P., and Shaw, P. (2007). Loss of imprinting and cancer. J. Pathol. *211*, 261–268.

Kalish, J.M., Jiang, C., and Bartolomei, M.S. (2014). Epigenetics and imprinting in human disease. Int. J. Dev. Biol. *58*, 291–298.

Kaneko, S., Son, J., Bonasio, R., Shen, S.S., and Reinberg, D. (2014). Nascent RNA interaction keeps PRC2 activity poised and in check. Genes Dev. *28*, 1983–1988.

Khoury, H., Suarez-Saiz, F., Wu, S., and Minden, M.D. (2010). An upstream insulator regulates DLK1 imprinting in AML. Blood *115*, 2260–2263.

Kobayashi, H., Suda, C., Abe, T., Kohara, Y., Ikemura, T., and Sasaki, H. (2006). Bisulfite sequencing and dinucleotide content analysis of 15 imprinted mouse differentially methylated regions (DMRs): paternally methylated DMRs contain less CpGs than maternally methylated. DMRs. Cytogenet. Genome Res. *113*, 130–137.

Koide, T., Moriwaki, K., Uchida, K., Mita, A., Sagai, T., Yonekawa, H., Katoh, H., Miyashita, N., Tsuchiya, K., Nielsen, T.J., and Shiroishi, T. (1998). A new inbred strain JF1 established from Japanese fancy mouse carrying the classic piebald allele. Mamm. Genome *9*, 15–19.

Kota, S.K., Llères, D., Bouschet, T., Hirasawa, R., Marchand, A., Begon-Pescia, C., Sanli, I., Arnaud, P., Journot, L., Girardot, M., and Feil, R. (2014). ICR noncoding RNA expression controls imprinting and DNA replication at the Dlk1-Dio3 domain. Dev. Cell *31*, 19–33.

Krijger, P.H.L., Geeven, G., Bianchi, V., Hilvering, C.R.E., and De Laat, W. (2020). 4C-seq from beginning to end: a detailed protocol for sample preparation and data analysis. Methods *170*, 17–32.

Langmead, B., and Salzberg, S.L. (2012). Fast gapped-read alignment with Bowtie 2. Nat. Methods *9*, 357–359.

Lee, J., Matsuzawa, A., Shiura, H., Sutani, A., and Ishino, F. (2018). Preferable in vitro condition for maintaining faithful DNA methylation imprinting in mouse embryonic stem cells. Genes Cells *23*, 146–160.

Lei, H., Oh, S.P., Okano, M., Jüttermann, R., Goss, K.A., Jaenisch, R., and Li, E. (1996). De novo DNA cytosine methyltransferase activities in mouse embryonic stem cells. Development *122*, 3195–3205.

Li, H., Handsaker, B., Wysoker, A., Fennell, T., Ruan, J., Homer, N., Marth, G., Abecasis, G., and Durbin, R.; 1000 Genome Project Data Processing Subgroup (2009). The sequence alignment/map format and SAMtools. Bioinformatics *25*, 2078–2079.

Li, Y., and Sasaki, H. (2011). Genomic imprinting in mammals: its life cycle, molecular mechanisms and reprogramming. Cell Res. *21*, 466–473.

Lienert, F., Wirbelauer, C., Som, I., Dean, A., Mohn, F., and Schübeler, D. (2011). Identification of genetic elements that autonomously determine DNA methylation states. Nat. Genet. *43*, 1091–1097.

Lin, S.P., Youngson, N., Takada, S., Seitz, H., Reik, W., Paulsen, M., Cavaille, J., and Ferguson-Smith, A.C. (2003). Asymmetric regulation of imprinting on the maternal and paternal chromosomes at the Dlk1-Gtl2 imprinted cluster on mouse chromosome 12. Nat. Genet. *35*, 97–102.

Liu, L., Luo, G.Z., Yang, W., Zhao, X., Zheng, Q., Lv, Z., Li, W., Wu, H.J., Wang, L., Wang, X.-J., and Zhou, Q. (2010). Activation of the imprinted Dlk1-Dio3 region correlates with pluripotency levels of mouse stem cells. J. Biol. Chem. *285*, 19483–19490.

Liu, Y., Pelham-Webb, B., Di Giammartino, D.C., Li, J., Kim, D., Kita, K., Saiz, N., Garg, V., Doane, A., Giannakakou, P., et al. (2017). Widespread mitotic bookmarking by histone marks and transcription factors in pluripotent stem cells. Cell Rep. *19*, 1283–1293.

Llères, D., Moindrot, B., Pathak, R., Piras, V., Matelot, M., Pignard, B., Marchand, A., Poncelet, M., Perrin, A., Tellier, V., et al. (2019). CTCF modulates allele-specific sub-TAD organization and imprinted gene activity at the mouse Dlk1-Dio3 and Igf2-H19 domains. Genome Biol. *20*, 272.

Luo, Z., Lin, C., Woodfin, A.R., Bartom, E.T., Gao, X., Smith, E.R., and Shilatifard, A. (2016). Regulation of the imprinted Dlk1-Dio3 locus by allele-specific enhancer activity. Genes Dev. *30*, 92–101.

Mandegar, M.A., Huebsch, N., Frolov, E.B., Shin, E., Truong, A., Olvera, M.P., Chan, A.H., Miyaoka, Y., Holmes, K., Spencer, C.I., et al. (2016). CRISPR interference efficiently induces specific and reversible gene silencing in human iPSCs. Cell Stem Cell *18*, 541–553.

Manodoro, F., Marzec, J., Chaplin, T., Miraki-Moud, F., Moravcsik, E., Jovanovic, J.V., Wang, J., Iqbal, S., Taussig, D., Grimwade, D., et al. (2014). Loss of imprinting at the 14q32 domain is associated with microRNA overexpression in acute promyelocytic leukemia. Blood *123*, 2066–2074.

Mendizabal, I., and Yi, S.V. (2016). Whole-genome bisulfite sequencing maps from multiple human tissues reveal novel CpG islands associated with tissue-specific regulation. Hum. Mol. Genet. *25*, 69–82.

Mo, C.F., Wu, F.C., Tai, K.Y., Chang, W.C., Chang, K.W., Kuo, H.C., Ho, H.N., Chen, H.F., and Lin, S.P. (2015). Loss of non-coding RNA expression from the DLK1-DIO3 imprinted locus correlates with reduced neural differentiation potential in human embryonic stem cell lines. Stem Cell Res. Ther. *6*, 1.

Morita, S., Noguchi, H., Horii, T., Nakabayashi, K., Kimura, M., Okamura, K., Sakai, A., Nakashima, H., Hata, K., Nakashima, K., and Hatada, I. (2016). Targeted DNA demethylation in vivo using dCas9-peptide repeat and scFv-TET1 catalytic domain fusions. Nat. Biotechnol. *34*, 1060–1065.

Morlando, M., and Fatica, A. (2018). Alteration of epigenetic regulation by long noncoding RNAs in cancer. Int. J. Mol. Sci. *19*, 570.

Nikolayeva, O., and Robinson, M.D. (2014). edgeR for differential RNA-seq and ChIP-seq analysis: an application to stem cell biology. Methods Mol. Biol. *1150*, 45–79.

Novitch, B.G., Chen, A.I., and Jessell, T.M. (2001). Coordinate regulation of motor neuron subtype identity and pan-neuronal properties by the bHLH repressor Olig2. Neuron *31*, 773–789.

Nowak, K., Stein, G., Powell, E., He, L.M., Naik, S., Morris, J., Marlow, S., and Davis, T.L. (2011). Establishment of paternal allele-specific DNA methylation at the imprinted mouse Gtl2 locus. Epigenetics *6*, 1012–1020.

Okano, M., Bell, D.W., Haber, D.A., and Li, E. (1999). DNA methyltransferases Dnmt3a and Dnmt3b are essential for de novo methylation and mammalian development. Cell *99*, 247–257.

Pachano, T., Sánchez-Gaya, V., Ealo, T., Mariner-Faulí, M., Bleckwehl, T., Asenjo, H.G., Respuela, P., Cruz-Molina, S., Muñoz-San Martín, M., Haro, E., et al. (2021). Orphan CpG islands amplify poised enhancer regulatory activity and determine target gene responsiveness. Nat. Genet. *53*, 1036–1049.

Paulsen, M., Takada, S., Youngson, N.A., Benchaib, M., Charlier, C., Segers, K., Georges, M., and Ferguson-Smith, A.C. (2001). Comparative sequence analysis of the imprinted Dlk1-Gtl2 locus in three mammalian species reveals highly conserved genomic elements and refines comparison with the Igf2-H19 region. Genome Res. *11*, 2085–2094.

Pelham-Webb, B., Polyzos, A., Wojenski, L., Kloetgen, A., Li, J., Di Giammartino, D.C., Sakellaropoulos, T., Tsirigos, A., Core, L., and Apostolou, E. (2021). H3K27ac bookmarking promotes rapid post-mitotic activation of the pluripotent stem cell program without impacting 3D chromatin reorganization. Mol. Cell *81*, 1732–1748.e8.

Plasschaert, R.N., and Bartolomei, M.S. (2014). Genomic imprinting in development, growth, behavior and stem cells. Development *141*, 1805–1813.

Quenneville, S., Turelli, P., Bojkowska, K., Raclot, C., Offner, S., Kapopoulou, A., and Trono, D. (2012). The KRAB-ZFP/KAP1 system contributes to the early embryonic establishment of site-specific DNA methylation patterns maintained during development. Cell Rep. *2*, 766–773.

Quenneville, S., Verde, G., Corsinotti, A., Kapopoulou, A., Jakobsson, J., Offner, S., Baglivo, I., Pedone, P.V., Grimaldi, G., Riccio, A., and Trono, D. (2011). In embryonic stem cells, ZFP57/KAP1 recognize a methylated hexanucleotide to affect chromatin and DNA methylation of imprinting control regions. Mol. Cell *44*, 361–372.

Rabinovitz, S., Kaufman, Y., Ludwig, G., Razin, A., and Shemer, R. (2012). Mechanisms of activation of the paternally expressed genes by the Prader-Willi imprinting center in the Prader-Willi/Angelman syndromes domains. Proc. Natl. Acad. Sci. USA *109*, 7403–7408.

Ran, F.A., Hsu, P.D., Wright, J., Agarwala, V., Scott, D.A., and Zhang, F. (2013). Genome engineering using the CRISPR-Cas9 system. Nat Protoc *8*, 2281–2308.

Raviram, R., Rocha, P.P., Müller, C.L., Miraldi, E.R., Badri, S., Fu, Y., Swanzey, E., Proudhon, C., Snetkova, V., Bonneau, R., and Skok, J.A. (2016). 4C-ker: a method to reproducibly identify genome-wide interactions captured by 4C-Seq experiments. PLoS Comput. Biol. *12*, e1004780.

Riso, V., Cammisa, M., Kukreja, H., Anvar, Z., Verde, G., Sparago, A., Acurzio, B., Lad, S., Lonardo, E., Sankar, A., et al. (2016). ZFP57 maintains the parent-of-origin-specific expression of the imprinted genes and differentially affects non-imprinted targets in mouse embryonic stem cells. Nucleic Acids Res. *44*, 8165–8178.

Robinson, J.T., Thorvaldsdóttir, H., Winckler, W., Guttman, M., Lander, E.S., Getz, G., and Mesirov, J.P. (2011). Integrative genomics viewer. Nat Biotechnol *29*, 24–26.

Rose, N.R., and Klose, R.J. (2014). Understanding the relationship between DNA methylation and histone lysine methylation. Biochim. Biophys. Acta *1839*, 1362–1372.

Saito, T., Hara, S., Kato, T., Tamano, M., Muramatsu, A., Asahara, H., and Takada, S. (2018). A tandem repeat array in IG-DMR is essential for imprinting of paternal allele at the Dlk1-Dio3 domain during embryonic development. Hum. Mol. Genet. *27*, 3283–3292.

Sánchez-Castillo, M., Ruau, D., Wilkinson, A.C., Ng, F.S., Hannah, R., Diamanti, E., Lombard, P., Wilson, N.K., and Gottgens, B. (2015). CODEX: a next-generation sequencing experiment database for the haematopoietic and embryonic stem cell communities. Nucleic Acids Res. *43*, D1117–D1123.

Sanli, I., Lalevée, S., Cammisa, M., Perrin, A., Rage, F., Llères, D., Riccio, A., Bertrand, E., and Feil, R. (2018). Meg3 non-coding RNA expression controls imprinting by preventing transcriptional upregulation in cis. Cell Rep. *23*, 337–348.

Sanmiguel, J.M., and Bartolomei, M.S. (2018). DNA methylation dynamics of genomic imprinting in mouse development. Biol. Reprod. *99*, 252–262.

Sato, S., Yoshida, W., Soejima, H., Nakabayashi, K., and Hata, K. (2011). Methylation dynamics of IG-DMR and Gtl2-DMR during murine embryonic and placental development. Genomics *98*, 120–127.

Schneider, C.A., Rasband, W.S., and Eliceiri, K.W. (2012). NIH Image to ImageJ: 25 years of image analysis. Nat Methods *9*, 671–675.

Semrau, S., Goldmann, J.E., Soumillon, M., Mikkelsen, T.S., Jaenisch, R., and Van Oudenaarden, A. (2017). Dynamics of lineage commitment revealed by single-cell transcriptomics of differentiating embryonic stem cells. Nat. Commun. *8*, 1096.

Shi, H., Strogantsev, R., Takahashi, N., Kazachenka, A., Lorincz, M.C., Hemberger, M., and Ferguson-Smith, A.C. (2019). ZFP57 regulation of transposable elements and gene expression within and beyond imprinted domains. Epigenetics Chromatin *12*, 49.

Stadtfeld, M., Apostolou, E., Akutsu, H., Fukuda, A., Follett, P., Natesan, S., Kono, T., Shioda, T., and Hochedlinger, K. (2010). Aberrant silencing of imprinted genes on chromosome 12qF1 in mouse induced pluripotent stem cells. Nature *465*, 175–181.

Stadtfeld, M., Apostolou, E., Ferrari, F., Choi, J., Walsh, R.M., Chen, T., Ooi, S.S., Kim, S.Y., Bestor, T.H., Shioda, T., et al. (2012). Ascorbic acid prevents

loss of Dlk1-Dio3 imprinting and facilitates generation of all-iPS cell mice from terminally differentiated B cells. Nat. Genet. *44*, 398–405, S1.

Stelzer, Y., Wu, H., Song, Y., Shivalila, C.S., Markoulaki, S., and Jaenisch, R. (2016). Parent-of-origin DNA methylation dynamics during mouse development. Cell Rep. *16*, 3167–3180.

Straussman, R., Nejman, D., Roberts, D., Steinfeld, I., Blum, B., Benvenisty, N., Simon, I., Yakhini, Z., and Cedar, H. (2009). Developmental programming of CpG island methylation profiles in the human genome. Nat. Struct. Mol. Biol. *16*, 564–571.

Strogantsev, R., Krueger, F., Yamazawa, K., Shi, H., Gould, P., Goldman-Roberts, M., Mcewen, K., Sun, B., Pedersen, R., and Ferguson-Smith, A.C. (2015). Allele-specific binding of ZFP57 in the epigenetic regulation of imprinted and non-imprinted monoallelic expression. Genome Biol. *16*, 112.

Swanzey, E., Mcnamara, T.F., Apostolou, E., Tahiliani, M., and Stadtfeld, M. (2020). A susceptibility locus on chromosome 13 profoundly impacts the stability of genomic imprinting in mouse pluripotent stem cells. Cell Rep. *30*, 3597–3604.e3.

Swanzey, E., and Stadtfeld, M. (2016). A reporter model to visualize imprinting stability at the Dlk1 locus during mouse development and in pluripotent cells. Development *143*, 4161–4166.

Takada, S., Paulsen, M., Tevendale, M., Tsai, C.E., Kelsey, G., Cattanach, B.M., and Ferguson-Smith, A.C. (2002). Epigenetic analysis of the Dlk1-Gtl2 imprinted domain on mouse chromosome 12: implications for imprinting control from comparison with Igf2-H19. Hum. Mol. Genet. *11*, 77–86.

Tucci, V., Isles, A.R., Kelsey, G., and Ferguson-Smith, A.C.; Erice Imprinting Group (2019). Genomic imprinting and physiological processes in mammals. Cell *176*, 952–965.

Vanzan, L., Soldati, H., Ythier, V., Anand, S., Braun, S.M.G., Francis, N., and Murr, R. (2021). High throughput screening identifies SOX2 as a super pioneer factor that inhibits DNA methylation maintenance at its binding sites. Nat. Commun. *12*, 3337.

Verma, N., Pan, H., Doré, L.C., Shukla, A., Li, Q.V., Pelham-Webb, B., Teijeiro, V., González, F., Krivtsov, A., Chang, C.-J., et al. (2018). TET proteins safeguard bivalent promoters from de novo methylation in human embryonic stem cells. Nat. Genet. *50*, 83–95.

Vojta, A., Dobrinić, P., Tadić, V., Bočkor, L., Korać, P., Julg, B., Klasić, M., and Zoldoš, V. (2016). Repurposing the CRISPR-Cas9 system for targeted DNA methylation. Nucleic Acids Res. *44*, 5615–5628.

Wang, Y., Shen, Y., Dai, Q., Yang, Q., Zhang, Y., Wang, X., Xie, W., Luo, Z., and Lin, C. (2017). A permissive chromatin state regulated by ZFP281-AFF3 in controlling the imprinted Meg3 polycistron. Nucleic Acids Res. *45*, 1177–1185.

Wichterle, H., Lieberam, I., Porter, J.A., and Jessell, T.M. (2002). Directed differentiation of embryonic stem cells into motor neurons. Cell *110*, 385–397.

Williams, K., Christensen, J., Pedersen, M.T., Johansen, J.V., Cloos, P.A., Rappsilber, J., and Helin, K. (2011). TET1 and hydroxymethylcytosine in transcription and DNA methylation fidelity. Nature *473*, 343–348.

Xu, X., Tao, Y., Gao, X., Zhang, L., Li, X., Zou, W., Ruan, K., Wang, F., Xu, G.L., and Hu, R. (2016). A CRISPR-based approach for targeted DNA demethylation. Cell Discov. *2*, 16009.

Ying, Y., Yang, X., Zhao, K., Mao, J., Kuang, Y., Wang, Z., Sun, R., and Fei, J. (2015). The Kruppel-associated box repressor domain induces reversible and irreversible regulation of endogenous mouse genes by mediating different chromatin states. Nucleic Acids Res. *43*, 1549–1561.

Yoon, B., Herman, H., Hu, B., Park, Y.J., Lindroth, A., Bell, A., West, A.G., Chang, Y., Stablewski, A., Piel, J.C., et al. (2005). Rasgrf1 imprinting is regulated by a CTCF-dependent methylation-sensitive enhancer blocker. Mol. Cell. Biol. *25*, 11184–11190.

Zhang, Y.W., Wang, Z., Xie, W., Cai, Y., Xia, L., Easwaran, H., Luo, J., Yen, R.C., Li, Y., and Baylin, S.B. (2017). Acetylation enhances TET2 function in protecting against abnormal DNA methylation during oxidative stress. Mol. Cell *65*, 323–335.

Zhao, J., Ohsumi, T.K., Kung, J.T., Ogawa, Y., Grau, D.J., Sarma, K., Song, J.J., Kingston, R.E., Borowsky, M., and Lee, J.T. (2010). Genome-wide identification of polycomb-associated RNAs by RIP-seq. Mol. Cell *40*, 939–953.

Zhao, Y., Sun, H., and Wang, H. (2016). Long noncoding RNAs in DNA methylation: new players stepping into the old game. Cell Biosci. *6*, 45.